BITLIS EREN UNIVERSITY
JOURNAL OF SCIENCE AND TECHNOLOGY

E-ISSN: 2146-7706

SYNTHESIS AND CHARACTERIZATION OF CHROMIUM-BASED CATALYSTS ON TITANIUM-MODIFIED-MCM-41 FOR OXIDATIVE DEHYDROGENATION OF ISOBUTANE

Hiba Mustafa Yousef Mosa [1], Meltem Dogan [2], Saliha Cetinyokus [3,*]

[1] *Gazi University, Department of Chemical Engineering, Turkey, hibamustafayousef.mosa@gazi.edu.tr*
[2] *Gazi University, Department of Chemical Engineering, Turkey, meltem@gazi.edu.tr*
[3] *Gazi University, Department of Chemical Engineering, Turkey, salihakilicarslan@gazi.edu.tr*
***** *Corresponding author*

KEYWORDS

MCM-41
Chromium-based catalysts
Hydrothermal stability
Oxidative dehydrogenation of isobutane

ARTICLE INFO

Research Article
DOI:
10.17678/beuscitech.1385177

Received	2 November 2024
Accepted	30 January 2024
Year	2024
Volume	14
Issue	1
Pages	1-22

ABSTRACT

This study aimed to prepare chromium-based catalysts on titanium-modified MCM-41 for oxidative dehydrogenation reactions. MCM-41 was synthesized hydrothermally. In order to increase the hydrothermal stability of support, titanium was added to the MCM-41. The titanium source (K_2TiF_6) was dissolved in two different solvents (hot water and sulfuric acid). The hydrothermal stability test was performed with the samples. The samples were characterized by XRD, N_2 adsorption/desorption, FT-IR, and SEM/EDS analysis. When titanium was added to the MCM-41 structure, it was determined that the pore walls thickened, and the main peak characterizing the hexagonal structure was preserved. With the modification, the average pore diameter of MCM-41 decreased from 28Å to 22Å, and the surface area decreased from 1250 m^2/g to 500 m^2/g. The hydrothermal stability test indicated that the loading of titanium improved the stability of MCM-41. FT-IR results showed that titanium has formed strong bonds with oxygen atoms, creating Si-O-Ti, Ti-OH, and Ti-O bonds. These bonds enhanced to stabilize the MCM-41 structure, making it more resistant to structural changes. Smaller crystal size (178Å) and higher surface area (554 m^2/g) were determined in the support prepared by dissolving the titanium source in hot water. Therefore, this support was used in catalyst synthesis. Chromium-based catalysts on titanium-modified MCM-41 were prepared by wet impregnation method at different chromium loading (3% and 10%, by mass). The presence of the anatase phase of TiO_2 and inactive α-Cr_2O_3 in the high chromium-loaded sample was determined. Therefore, catalytic tests were carried out with a catalyst containing 3% chromium by mass, prepared using a Ti-modified support, as well as a catalyst prepared using an unmodified support. The highest isobutane conversion (94%) and isobutene selectivity (81%) values were obtained for catalyst supported on Ti-modified MCM-41. High activity predicted for catalyst supported on modified MCM-41 was explained by improving hydrophilic properties.

1 INTRODUCTION

Around 30 years ago, mesoporous MCM-41 materials were discovered and have been widely used in many applications, such as catalysis, adsorption, and separation technology [1]- [3]. MCM-41 has been extensively reported due to the high surface area (up to 1000 m2/g) and tailored mesoporous sizes (~10 nm) [4]. MCM-41 preparation method requires four ingredients: a silicate source, a surfactant molecule, acid, and water. The silica species that arise from the hydrolysis of the silicate source are negatively charged and are then attracted to the positively charged ammonium groups of the cationic surfactant [5], [6]. Cetyl Trimethyl Ammonium Bromide (CTAB) is the most often used surfactant in the synthesis. The surfactant is removed to reveal the mesoporous channels. There are different methods for removing the organic surfactant, such as solvent extraction or removal of physically adsorbed surfactants [7], electrochemical procedure [8], and UV/ozone irradiation [9]. However, the most widely used technique is burning organic templates in an air or oxygen atmosphere. This process generates surface silanol groups (≡Si-OH), as well as the formation of some fused siloxane bridges. However, the removal of the surfactant, coupled with the presence of an amorphous silica structure, leads to low structural stability for these mesoporous silicas [10]. The limited hydrothermal stability of MCM-41 refers to its susceptibility to damage from thermal treatments involving water, steam, or a combination of both. Bezerra et al. reported a systematic study on MCM-41 synthesized at various temperatures to relevant structural order of mesoporous silica under humidity. It was found that the stability of MCM-41 relied on pore wall thickness and the quantity of Si-OH groups when MCM-41 was exposed to humidity, water physisorption occurred, leading to a loss of structural order due to hydrolysis of siloxane bond [11]. A recent study by Perez et al. suggested that capillarity led to loss of ordering and structural damage of MCM-41 at moderate hydrothermal treatment temperatures in water, associated with hydrolysis and decreased mechanical strength [12].

Various methods have been developed to enhance the hydrothermal stability of MCM-41 materials, such as adding surfactant templates, using stable silica sources/precursors, grafting aluminum onto pure silica, creating thicker pore walls, eliminating silanol groups, and promoting silanol group condensation through salt or

hydrothermal structure-directing agents [12], [13]. Incorporating metal cations, such as Ti, Al, Cr, Zr, V, Mo, Cu, Ni, Co, and Fe, into the MCM-41 silica framework via controlled synthesis or post-synthesis modification enhances its catalytic properties and helps in overcoming the disadvantages mentioned above [3], [14]-[16]. Recently, the use of MCM-41 modified with Ti and Ti oxides has gained great attention in the industry. Due to its catalytic properties, it is widely used in basic catalytic processes such as environmental catalysis, petrochemical and refinery catalysis, olefin epoxidation, and biomass conversion [3], [17], [18]. Sekkiou et al. showed that Cu-MCM-41 exhibited low hydrothermal stability due to the addition of copper and the formation of CuO oxide; in contrast, Cu-Al-MCM-41 demonstrated high hydrothermal stability attributed to the presence of aluminum and an ion exchange process [19]. Chao et al. found that intercalation of the CuAAPTS complex improved hydrothermal stability by creating highly cross-linked silica "pillars" through covalent bonding [20]. Song et al. reported that pre-treatment with (NH4)2SiF6 improved hydrothermal stability by repairing surface defects and replacing some silicon hydroxyls with F-ions [21]. Jiang et al. showed that MCM-41 with Si/Al: 25 maintained its mesoporous structure even after a 12-hour hydrothermal stability test in boiling water due to the loading of the Al atom. This demonstrated that the hydrothermal stability of MCM-41 can be enhanced by secondary restructure with a pore diameter larger than 3.3 nm and a BET surface area exceeding 800 m^2/g [22].

Chromium-based catalysts are widely used in dehydrogenation reactions. Catalytic activity is high when the (+6) valence oxides of chromium are present in the catalyst structure. It was shown that the crystal size highly influenced the catalytic activity [23], [24]. Cr-based catalysts supported on Ti-doped MCM-41 materials exhibit improved structural properties. A study by Al-Awadi et al. stated that TiO2 modification of MCM-41 increased the stability [25]. Wan et al. confirmed that titanium loading in a Cr-based catalyst reduced hydrophobicity due to Si-Ti bond formation [26]. It was reported that titanium coating on the catalyst surface as a metal oxide produced a protective effect, preventing the leaching of the active species during the reaction [27].

The aim of this study was to synthesize chromium-based catalysts supported on titanium-modified MCM-41 for oxidative dehydrogenation of isobutane. It was predicted that the titanium modification positively improved hydrothermal stability

and active species distribution. Catalysts were prepared by wet impregnation method at different chromium loading (3% and 10%, by mass). It was decided to carry out the catalytic test with the catalyst containing 3% chromium by mass because of the low crystal size and high surface area. A catalyst was also prepared using an unmodified support to observe the effect of modification with titanium on catalytic activity.

2 EXPERIMENTAL

2.1 Synthesis of MCM-41 and Titanium-Modified-MCM-41

MCM-41 mesoporous silica was synthesized using $C_{19}H_{42}BrN$ (N-cetyl-N, N, N-trimethyl ammonium bromide) as surfactant and sodium silicate solution (composed of 27% SiO_2, 8% Na_2O, and 65% H_2O by mass) as the silica source. The synthesis was carried out with a surfactant/Si ratio of 0.5 (mole/mole). Firstly, the surfactant was dissolved in deionized water and stirred at 30°C until a clear solution was obtained. Then the sodium silicate solution was added dropwise under stirring. The resulting mixture's pH was adjusted to 11 before being placed in a Teflon-lined stainless-steel autoclave, where it was kept at 120°C for 96 hours. After removing the sample from the autoclave, it was washed, dried, and calcined in a dry air flow (135 ml/min) at 600°C for 6 hours.

To modify MCM-41, K_2TiF_6 (dipotassium hexafluorotitanate) was used as a titanium source. In the synthesis of titanium-modified MCM-41, the same method described above was followed in the synthesis of pure MCM-41. In the step where sodium silicate solution was added, the dissolved titanium source was added alternately with the silica source. The titanium source was dissolved in two different solvents (hot water and sulfuric acid). The synthesized samples were labeled as TiW-M (K2TiF6 dissolved in hot water) and TiA-M (K_2TiF_6 dissolved in acid).

The hydrothermal stability test was carried out for pure MCM-41 and samples of MCM-41 modified with titanium. First, the samples were put in 30 mL water and heated to 383K for 5 hours under gentle stirring. The amount of water was kept constant by adding hot water when needed. After this treatment, the remaining samples were filtered and dried at room temperature. Hydrothermally treated samples were named by writing "HT" at the end of their names.

2.2 Preparation of Chromium-Based Catalysts

In the catalyst preparation studies, chromium-based catalysts supported on titanium-modified MCM-41 were prepared by wet impregnation method with Cr(NO3)3.9H2O (chromium nitrate) as the chromium source. Chromium metal loading on the titanium-modified MCM-41 was planned to be 3% and 10% by mass, and titanium metal loading was kept constant at 2.5 % by mass. Deionized water was mixed with titanium-modified MCM-41, and then the dissolved chromium nitrate salt was added to the mixture drop by drop at 40°C. Then the mixture's temperature was raised to 60°C to evaporate the water followed by drying at 100°C. The prepared catalyst was calcined at 600°C for 6 hours with a dry air flow rate of 135 ml/min. The final obtained catalysts were denoted as xCr@Ti-MCM-41, where x represents the mass percentages of Cr. Using the impregnation method described above, the 3Cr@MCM-41 catalyst was also prepared using unmodified MCM-41.

2.3 Catalytic Tests

The activity of chromium-based catalysts used in the oxidative dehydrogenation of isobutane is highly affected by the crystal size, where the catalyst containing a smaller chromium crystal size shows better activity [28]. For this reason, it was decided to carry out the catalytic test studies with a 3Cr@Ti-MCM-41 catalyst, which had a smaller chromium crystal size. Catalytic test studies were also carried out with catalyst supported on unmodified MCM-41 (3Cr@MCM-41). The experimental setup used for the oxidative dehydrogenation of isobutane is given in Figure 1.

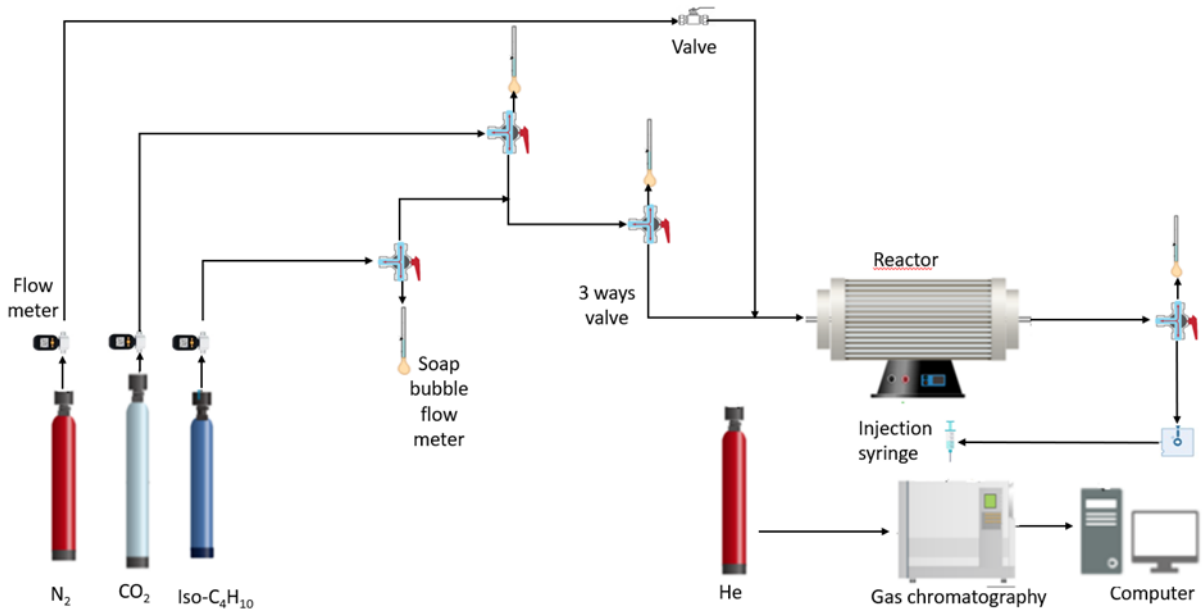

***Figure 1**. Experimental setup used for the catalytic tests*

The catalytic tests were carried out in a quartz reactor (diameter: 0.65cm, length: 1cm) with a catalyst loading of 0.1 grams. The experiment was carried out at a temperature of 600℃ and under atmospheric pressure for 2 hours. The feed, consisting of isobutane and carbon dioxide (i-C_4H_{10}/CO_2 feed ratio: 1/5), was fed to the reactor at a total flow rate of 50 ml/min (WHSV: 51 h^{-1}). The gas samples collected at specific time intervals from the reactor outlet were analyzed using a gas chromatography instrument (SRI 8610C) equipped with a silica column. The isobutane conversion and isobutene selectivity values were determined from the following equations (Eq.1 and Eq.2).

$$Isobutane\ conversion\ (\%) = \frac{(i\text{-}C_4H_{10,initial} - i\text{-}C_4H_{10,exit})}{(i\text{-}C_4H_{10,initial})} \times 100 \quad \textbf{(1)}$$

$$Isobutene\ selectivity\ (\%) = \frac{(i\text{-}C_4H_{8,exit})}{(i\text{-}C_4H_{10,initial} - i\text{-}C_4H_{10,exit})} \times 100 \quad \textbf{(2)}$$

2.4 Characterization Studies

2.4.1 XRD

XRD patterns of MCM-41 supports and catalysts were performed using a Rigaku instrument (D/MAX N2200) with Cu, Kα irradiation source (λ= 1.5406Å). Small angle profiles (2θ range: 1-10°) were used to determine the characteristic peaks of MCM-41, while wide angle profiles (2θ range: 10-80°) were used to identify distinct crystalline formations in metal-incorporated materials.

N_2 adsorption/desorption

The BET surface areas, pore size distribution, and pore volumes of the samples were determined through N_2 adsorption/desorption using the Quantochrome (Autosorp 6) physical adsorption device after degassing the samples at 250°C for 2 hours. Pore size distributions were analyzed using the Barrett Joyner–Halenda (BJH) model from the branch of the adsorption profiles of isotherms.

2.4.2 SEM/EDS

SEM/EDS analyses were conducted using a QUANTA (400F Field Emission) high-resolution Scanning Electron Microscope (SEM). SEM photographs were used to analyze the samples' morphology, while EDS analyses determined the compositions of the samples.

2.4.3 FT-IR

Fourier Transform Infrared Spectrophotometer (Jasco FT-IR 4700) analyses were performed to identify the chemical bonds present in the Ti-modified MCM-41 structure.

3 RESULTS AND DISCUSSIONS

3.1 Characterization Studies of the Supports

Hydrothermal stability tests were performed to determine the water dissolution behavior of the unmodified and Ti-modified MCM-41. In this section, the results of the characterization studies carried out before and after the hydrothermal stability tests are presented.

Before Hydrothermal Stability Tests

XRD diffraction patterns of unmodified MCM-41 and titanium-modified MCM-41 before the hydrothermal stability test are given in Figure 2.

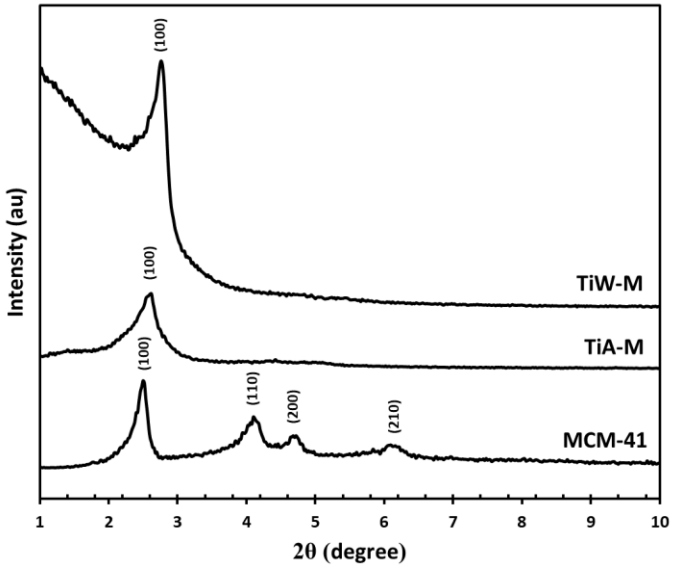

Figure 2*. XRD Patterns of the catalyst supports before the hydrothermal stability test*

The XRD pattern for the unmodified MCM-41 displayed four peak positions (100, 110, 200, and 210 reflections) from 1° to 10°, confirming the typical MCM-41 structure [28]. For the modified MCM-41 with titanium, only the 100 reflection peak was observed, which showed that the hexagonal structure was preserved. In the literature, when metal was added to the MCM-41 structure, the disappearance of the peaks in the (110), (200), and (210) planes indicated that the hexagonal pore structure was preserved despite the disordered structure [29]. Additionally, it was observed that the detected peak shifted to a higher 2θ when titanium was loaded into the MCM-41 structure. This decrease in interplanar d100 spacing resulted from incorporating Ti atoms rather than Si atoms into the MCM-41 structure. The low peak intensity seen for the TiA-M sample indicated the formation of a lamellar phase, which was thought to cross-link and then transform the hexagonal phase [30].

N_2 adsorption/desorption analyses were carried out for unmodified MCM-41 and modified MCM-41 supports. The N_2 adsorption/desorption isotherms and pore size distribution are shown in Figure 3. Structural properties determined from physical adsorption and XRD data are given in Table 1.

Figure 3. N_2 adsorption/desorption isotherms and pore size distributions for the TiW-M and TiA-M support materials.

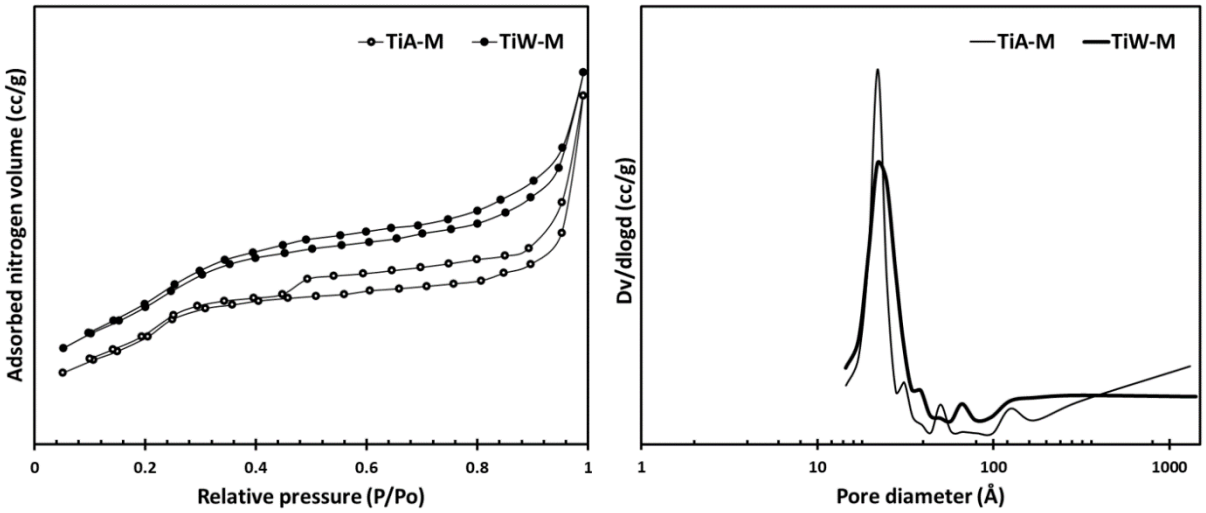

***Figure 3**. N_2 adsorption/desorption isotherms and pore size distributions for the TiW-M and TiA-M support materials*

***Table 1**. Structural properties of the support materials*

Sample	d, Å	δ, Å	L, Å	Surface area (BET) m^2/g	Pore volume cc/g	Pore diameter Å
MCM-41	28	13	-	1250	1.20	28
TiW-M	32	15	178	554	0.59	22
TiA-M	34	18	204	473	0.57	22

d: distance between layers *δ: wall thickness* *L: crystal size*

It can be seen that both TiW-M and TiA-M samples exhibited typical MCM-41 isotherm characteristics, classified as Type IV and Hysteresis I according to IUPAC classification. Type IV isotherm confirmed the presence of the mesoporous structure, while Hysteresis I indicated a regular and homogeneous formed structure with narrow pore sizes [31]. The absence of a step increase in volume at low relative pressure indicated no microspores in the modified material. Monolayer adsorption of nitrogen molecules occurred on the surface at low relative pressure values (P/Po < 0.2). As relative pressure increased, hysteresis formation and increased adsorption volume after 0.1 (P/Po) showed capillary condensation inside the mesoporous. At close-to-saturation, relative pressure (approaching 1), mesoporous were fully saturated,

while macrospores were partially saturated [32]. Meanwhile, for the TiA-M sample, the existence of ink-bottle pores can be discarded since the desorption branch showed a gentle decrease in the P/Po around 0.45–0.5. BJH adsorption pore size distribution was used to determine the pore diameter of prepared materials. The average mesoporous diameter of TiA-M was found to be identical to TiW-M, measuring 22 Å. It was observed that the surface area and pore volume of the titanium-modified supports decreased when compared to the unmodified MCM-41. This case can be explained by the presence of highly dispersed titanium species blocking the pores of the structure. The pore diameter for MCM-41 (28 Å) was still within the range generally observed for the MCM-41 material [28].

As a result of the data obtained from XRD and N_2 adsorption/desorption analysis, there was no significant difference in the structural and physical properties of the modified MCM-41 samples. A decrease in band gap energy was observed with titanium loading due to an increase in TiO_2 crystal size. Therefore, small crystal sizes were preferred in the literature [33]. The small crystal size may be attributed to the higher surface area, which prevents agglomeration of particles and leads to uniform dispersion of titanium oxide crystals. For this reason, it was decided to use the TiW-M sample with a smaller crystal size and higher surface area in catalyst preparation. FT-IR analyses of the TiW-M support were conducted, and the obtained spectrum is given in Figure 4.

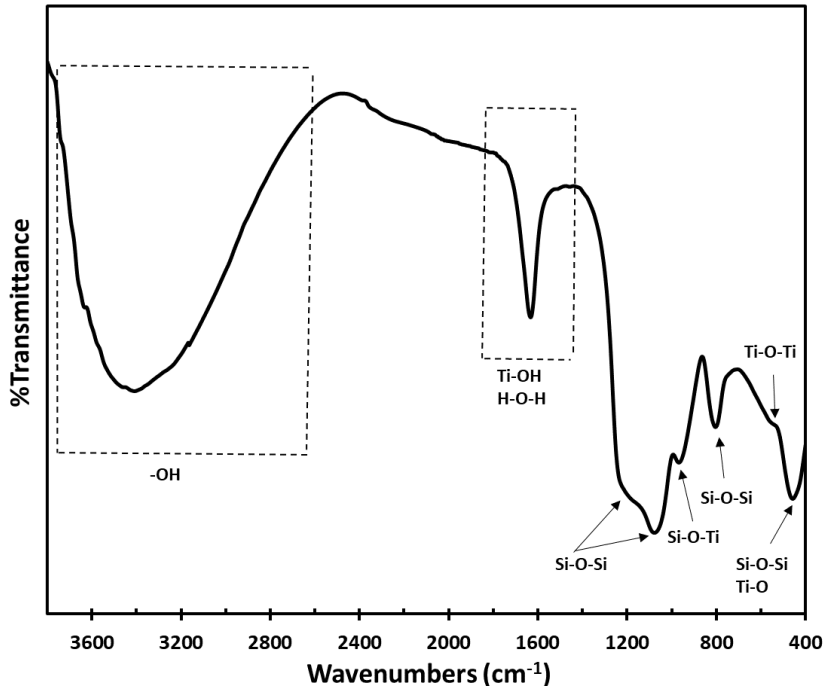

***Figure 4**. FT-IR spectra of Ti-modified MCM-41*

The 3440 cm^{-1} band is associated with the presence of hydroxyl groups (-OH) on the framework. The band at a range of 1645 cm^{-1} corresponds to bending vibrations of the Ti-OH and H-O-H. The band within the 1000–1245 cm^{-1} range is assigned to the presence of Si–O–Si bonds, which are inherent to the siliceous structure and serve as a distinctive characteristic. The band at 800 cm^{-1} is also related to the bending vibrations of the Si–O–Si groups. The presence of the 960 cm^{-1} band in the materials is associated with the isomorphic substitution of Si by Ti ions and is attributed to the stresses of the Si–O–Ti polar bonds [30], [34]. The absorption peak at 690 cm^{-1} is associated with the infrared vibrations of Ti-O in the anatase phase [35]. The bands at 455 cm^{-1} are ascribed to the bending vibrations of the Si–O–Si groups and Ti-O metal oxides.

After Hydrothermal Stability Tests

MCM-41 supports were modified with titanium to increase hydrothermal stability. The XRD patterns of the prepared supports after the hydrothermal stability test are presented in Figure 5.

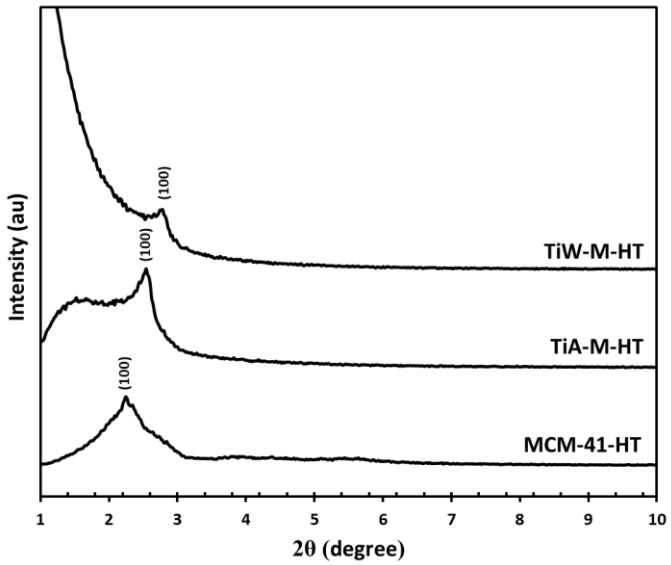

***Figure 5**. XRD Patterns of the supports after the hydrothermal stability test*

When Figure 2 and Figure 5 are compared, it can be seen that MCM-41 material shows a structural change after the hydrothermal stability test. According to sample dissolution data, unmodified MCM-41 dissolved in water approximately 9 times more than the Ti-modified support.

XRD patterns revealed structural changes, reducing the main 100-reflection peak intensity for all MCM-41-supported materials after hydrothermal treatment. Unmodified MCM-41 lost the 110, 200, and 210 reflection peaks at 383K. This observation agreed with the literature [36]. The observed structural changes and dissolution data differences between unmodified MCM-41 and titanium-modified MCM-41 after hydrothermal treatment at 383K can be explained based on the inherent bonds in each material and their interactions with water.

MCM-41 contains Si-O-Si bonds in its framework, forming a highly ordered mesoporous structure that can collapse under hydrothermal conditions. In contrast, titanium-modified MCM-41 includes Ti-O-Si bonds resulting from the incorporation of titanium. These bonds are believed to enhance structural stability due to the strong nature of Ti-O bonds. The formation of the Si-O-Ti bond is suggested to have an impact on the prevention of sinterization [37]. Considering water-surface interactions, the hydrothermal exposure of MCM-41 resulted in a significant increase in water adsorption, which was mostly attributed to the presence of Silanol (Si-OH) groups that caused structural damage as water molecules interacted with surface hydroxyl groups. On the other hand, in titanium-modified MCM-41, the presence of Ti-OH and Ti-O-Si bonds probably influenced water adsorption dynamics. The interaction mechanism of Ti-OH with water was different from that of Si-OH, affecting the extent of structural changes. Liu et al. [36] stated that the water adsorption in MCM-41 material shifts from surface adsorption to multilayer adsorption. Also, due to hydrogen bonding, droplets are formed, and capillary condensation further occurs in the pores. Titanium can form strong bonds with oxygen atoms, creating Ti-OH and Ti-O bonds. These bonds contribute to the stabilization of the material's structure, making it more resistant to structural changes even in the presence of water at elevated temperatures [38]. Ti-O bonds tend to be stronger than Si-O bonds, which might contribute to the hydrothermal stability observed in modified MCM-41. It was shown by FT-IR analysis that Ti-OH, Ti-O, and Si-O-Ti bonds, the advantages of which were described in the literature, were present in the prepared support (Figure 4). Consistent with the literature, the hydrothermal stability of the Ti-modified support can be explained by the presence of these bonds.

3.2 Characterization Studies of Chromium-Based Catalysts

In the preparation of chromium-based catalysts, support (TiW-M), which was determined to have a smaller crystal size and higher surface area, was used. The XRD patterns of the synthesized catalysts supported on titanium-doped MCM-41 with different chromium loading (3% and 10% by mass) synthesized by impregnation methods are presented in Figure 6.

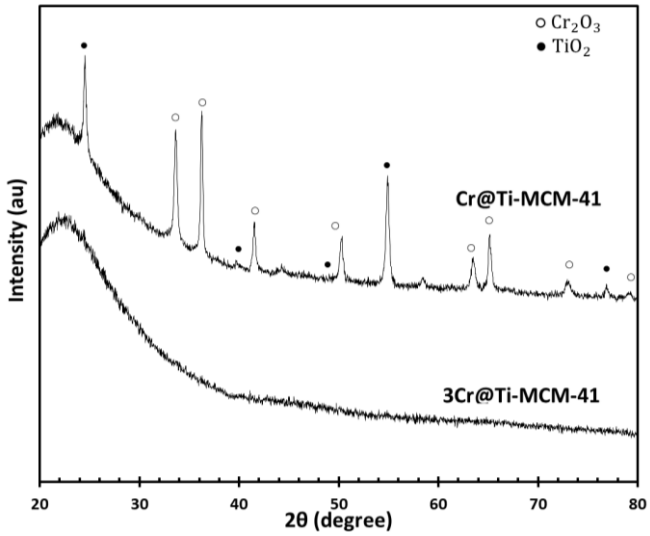

***Figure 6**. XRD Patterns of Chromium-based Catalysts.*

For 3Cr@Ti-MCM-41, a wider peak was observed at 22°, a distinctive feature of the amorphous silica structure. No peaks corresponding to chromium oxide were observed corresponding to the lower chromium content; this could indicate that these particles, if exist, were in an amorphous state or clusters/particles too small to be detected by XRD. As proven by the XRD results in Figure 6, nine peaks (at 2θ: 33.57°, 36.19°, 41.50°, 50.23°, 58.46°, 63.43°, 65.09°, 72.79°, and 79.10°) are observed in the pattern of 10Cr@Ti-MCM-41, which indexed to crystal rhombohedral α-Cr_2O_3 phase (JCPDS 00-006-0504). Also, from the reference patterns, the peaks at 2θ: 24.45°, 39.62°, 54.81°, and 76.83° indexed the TiO_2 anatase phase (JCPDS No.21–1272). The structural properties of the catalysts are given in Table 2.

***Table 2**. Structural properties of the prepared catalysts*

Catalyst	d(Å)	L (Å) Cr	L (Å) Ti	Surface area (BET) m^2/g
3Cr@Ti-MCM-41	3.90	9.40	-	440
10Cr@Ti-MCM-41	2.70	259	278	352

d: distance between layers δ: wall thickness L: crystal size

No significant change was observed in the surface area values of the synthesized catalysts.

SEM/EDS analysis was carried out on synthesized chromium-based catalysts to determine catalyst morphology and composition. SEM photographs are given in Figure 7.

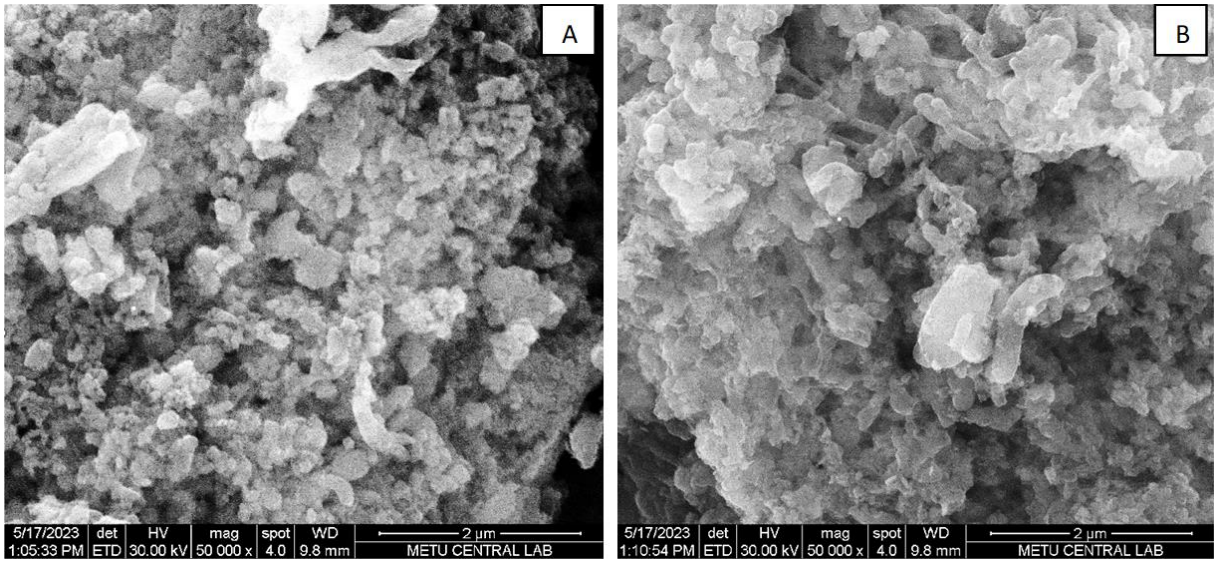

Figure 7*.SEM photographs of the catalysts:3Cr@Ti-MCM-41 (A),10Cr@Ti-MCM-41 (B)*

SEM images in Figure 7 confirm the homogeneous structure of the catalysts, the highly ordered structure of the MCM-41 support and the surface with a smooth appearance. It was shown that the incorporation of the metal oxides into the mesoporous was successful. Additionally, it was observed that catalysts containing 10% Cr by mass exhibited larger pores. Surface compositions of the chromium-based catalysts by EDS analysis are listed in Table 3.

Table 3*. Surface compositions of the chromium-based catalysts*

Element / Catalyst	Oxygen (O)	Sodium (Na)	Silica (Si)	Potassium (K)	Titanium (Ti)	Chromium (Cr)	Cr/Ti (mass/mass)
3Cr@Ti-MCM-41	58.39	1.31	35.10	0.46	2.18	2.56	1.17
10Cr@Ti-MCM-41	56.52	0.75	32.73	0.69	1.73	7.59	4.38

The amounts of chromium with EDS analysis were predicted as 2.56 and 7.59 (%, by mass), respectively, for 3Cr@Ti-MCM-41 and 10Cr@Ti-MCM-41. Lower chromium amounts were determined by EDS analysis than the chromium amounts (3%

Cr and 10% Cr, by mass) adjusted in the synthesis. This can be explained by the inability to detect chromium embedded in the pore walls of the support by EDS analysis. Similar results were reported in many studies in the literature [3], [39]. Cr/Ti ratios in the synthesis for 3% Cr and 10% Cr were 1.2 and 4, respectively. It can be seen that the Cr/Ti ratios determined from EDS and adjusted in the synthesis were very close to each other.

The 3Cr@MCM-41 catalyst containing 3% chromium by mass was also prepared using unmodified MCM-41 based on the same synthesis procedure. From XRD analysis Cr@MCM-41, the distances between layers (d) and the crystal size (L) were determined as 3.5 Å and 7.3 Å, respectively. from XRD analysis. The surface area (BET) of Cr@MCM-41 was obtained as 400 m^2/g from N_2 adsorption/desorption data.

3.3. Catalytic Tests

Oxidative dehydrogenation of isobutane in the presence of carbon dioxide was conducted over 3Cr@Ti-MCM-41 and 3Cr@MCM-41 catalysts. Isobutane conversion and isobutene selectivity values are shown in Figure 8 and Figure 9, respectively.

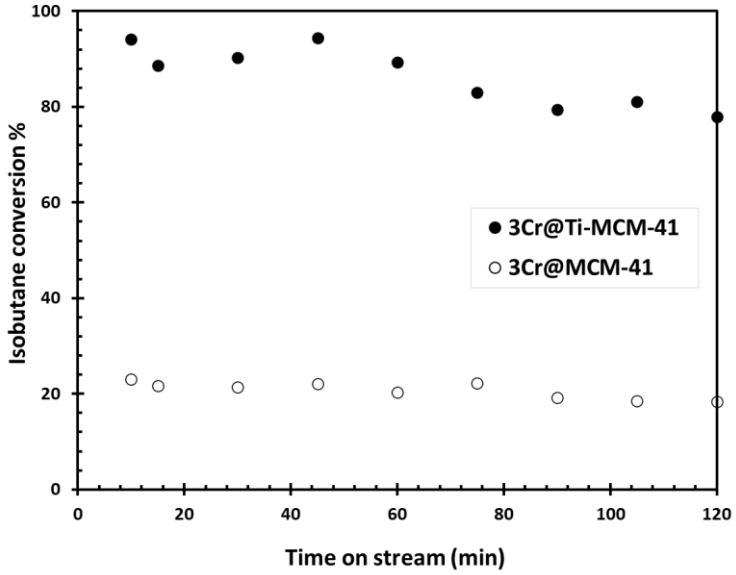

***Figure 8**. Isobutane conversion values (isobutane/CO_2 feed ratio: 1/5, 600℃, WHSV: 51 h^{-1})*

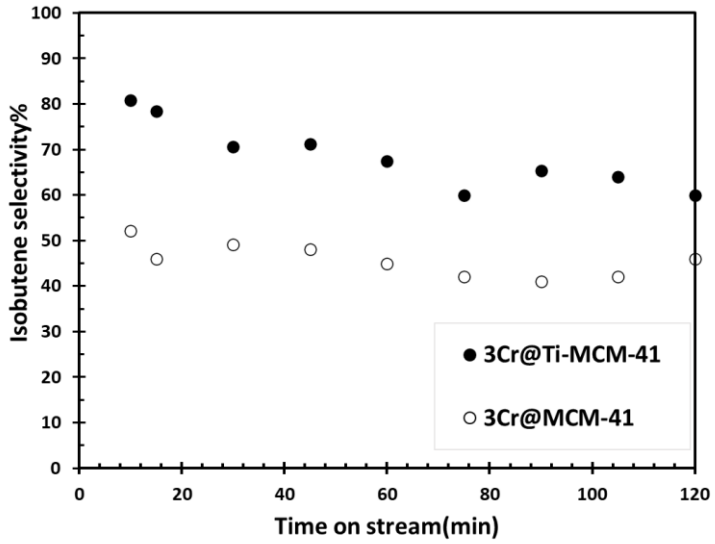

***Figure 9**. Isobutene selectivity values (isobutane/CO_2 feed ratio: 1/5, 600℃, WHSV: 51 h^{-1})*

As can be seen from Figure 8, isobutane conversion values obtained for 3Cr@Ti-MCM-41 are significantly higher (about 4 times) than that of the 3Cr@MCM-4 catalyst. It was emphasized in section 3.1 that the structural properties (such as surface area value and crystal size) of the 3Cr@Ti-MCM-41 and 3Cr@MCM-41 catalysts were similar. The high difference between the conversions can be explained by the modification of the support. The equilibrium conversion (Gaseq Program) was determined to be 46% at 600°C for a feed ratio of isobutane to CO_2 of 1 to 5 (mol). It can be seen that the conversion values over the 3Cr@MCM-4 catalyst were 50% less than the equilibrium conversion, while the conversion over 3Cr@Ti-MCM-41 exceeded the equilibrium conversion.

A recent study confirmed that the loading of titanium improved catalyst stability when compared to titanium-free catalysts [26]. It was established that doping Ti to MCM-41 significantly modified the structural properties and decreased hydrophobicity. According to the literature, three possible mechanisms can cause a reduction in hydrophobicity when titanium is added. These mechanisms are surface functionalization, surface charge modification, and structural rearrangement [30], [37]. Titanium species bond with Silanol groups (Si-OH) on MCM-41's surface. This case forms hydrophilic groups (like Ti-OH and Ti-O) that interact with water molecules through hydrogen bonding and reduce surface hydrophobicity. The existence of the hydrophilic groups was demonstrated by FT-IR analyses (Figure 4).

It was thought that the presence of hydrophilic groups helped the adsorption of water produced from the oxidative dehydrogenation reaction (Eq. 3).

$$i\text{-}C_4H_{10} + CO_2 \leftrightarrow i\text{-}C_4H_8 + H_2O + CO \quad \textbf{(3)}$$

The activity of chromium-based catalysts in dehydrogenation reactions is significantly affected by the number of mono-chromates in the structure [40]. It was reported that the transformation of di-chromates (Eq.4) to monochromates during the reaction occurred in the presence of water [39].

$$H_2O + Cr_2O_7^{2-} \leftrightarrow 2CrO_4^{2-} + 2H^+ \quad \textbf{(4)}$$

It can be said that the reason for the high conversion values over 3Cr@Ti-MCM-41 catalysts is the higher hydrophilicity achieved by loading Ti. When the selectivity values shown in Figure 9 are examined, it is seen that the 3Cr@Ti-MCM-41 catalyst have the higher selectivity values (60-81%). The appearance of propane, propene, and methane at the reactor outlet during the reaction showed that the following side reactions (Eq. 5 and Eq. 6) took place in both catalysts, more in the 3Cr@MCM-41 catalyst.

$$i\text{-}C_4H_{10} \leftrightarrow C_3H_6 + CH_4 \quad \textbf{(5)}$$

$$i\text{-}C_4H_{10} + H_2 \leftrightarrow C_3H_8 + CH_4 \quad \textbf{(6)}$$

4 CONCLUSIONS

New chromium-based catalysts supported on titanium-modified MCM-41 were synthesized by the impregnation method for oxidative dehydrogenation of isobutane. Hydrothermal stability tests showed that modified MCM-41 resisted structural changes even in the presence of water at high temperatures, unlike unmodified MCM-41. The hydrothermal stability provided by the addition of titanium was explained by the formation of Ti-O-Si, Ti-O, and Ti-OH bonds that strengthened the structure. The interactions between these bonds and water molecules influenced water adsorption behavior. MCM-41 maintained its hexagonal structure even after adding

chromium and titanium into the mesoporous structure. The inactive α-Cr_2O_3 form for the reaction was observed at high Cr-loading. The catalytic tests showed that chromium-based catalysts supported on titanium-modified-MCM-41 exhibited much higher conversion and selectivity values than the catalyst supported on unmodified MCM-41. This case was explained by the improved hydrophilic properties. Hydrophilic groups (Ti-OH and Ti-O) interacted with water molecules through hydrogen bonding and reduced surface hydrophobicity. The most active chromate type in chromium-based catalysts used in oxidative dehydrogenation reactions is monochromates. As the reaction progressed, monochromates turned into dichromates. It was thought that with the help of water adsorbed on the surface, dichromates turned into active monochromates again for catalysts supported on Ti-MCM-41. It can be said that the synthesized new catalyst is a good candidate that can be used in oxidative dehydrogenation reactions with its good hydrothermal stability, suitable textural properties and catalytic properties.

Conflict of Interest

There is no conflict of interest between the authors.

Authors Contributions

Hiba Mustafa Yousef Mosa: Collected the data. Performed the analysis.

Meltem Dogan: Conceived and design the analysis. Wrote the paper.

Saliha Cetinyokus: Contributed data or analysis tools.

Acknowledgment and Support

The authors would like to thank Gazi University Academic Writing Application and Research Center for proofreading the article.

Statement of Research and Publication Ethics

The study is complied with research and publication ethics.

REFERENCES

[1] S. Çetinyokuş, M. Doğan and Z. Erol, "Investigation of the effectiveness of Cr@MCM-41 catalysts in isobutane dehydrogenation," *Journal of the Faculty of Engineering and Architecture of Gazi University*, vol. 36, no. 2, pp. 1075-1088, 2021.

[2] Y. Chen, J. Lyu, Y. Wang, T. Chen and Y. Tian, "Synthesis, characterization, adsorption, and isotopic separation studies of pyrocatechol-modified MCM-41 for efficient boron removal," *Industrial & Engineering Chemistry Research*, vol. 58, no. 8, pp. 3282-3292, Feb. 2019, doi: 10.1021/acs.iecr.8b04748.

[3] T.H. Liou, S.M. Liu and G.W. Chen, "Utilization of e-wastes as a sustainable silica source in synthesis of ordered mesostructured titania nanocomposites with high adsorption and photoactivity," J*ournal of Environmental Chemical Engineering*, vol. 10, no. 2, 2022, doi: 10.1016/j.jece.2022.107283.

[4] W.Y. Sang and O.P. Ching, "Tailoring MCM-41 mesoporous silica particles through modified sol-gel process for gas separation," in AIP Conference Proceedings, 2017, vol. 1891, no. 1: AIP Publishing.

[5] B. Szczesniak, J. Choma and M. Jaroniec, "Major advances in the development of ordered mesoporous materials," *Chemical Communications*, vol. 56, no. 57, pp. 7836-7848, Jul. 2020, doi: 10.1039/d0cc02840a.

[6] C.S. Ha, S.S. Park, C.S. Ha, and S.S. Park, "General synthesis and physico-chemical properties of mesoporous materials," Periodic Mesoporous Organosilicas: Preparation, Properties and Applications, pp. 15-85, 2019

[7] S. C. Buratto, E. Latocheski, D.C.D. Oliveira and J. B. Domingos, "Influence of the capping agent PVP of the outer layer of Pd nanocubes surface on the catalytic hydrogenation of unsaturated C− C bonds," *Journal of the Brazilian Chemical Society*, vol. 31, pp. 1078-1085, 2020.

[8] I. Safo and M. Oezaslan, "Electrochemical cleaning of polyvinylpyrrolidone-capped Pt nanocubes for the oxygen reduction reaction," *Electrochimica Acta*, vol. 241, pp. 544-552, 2017.

[9] R.Y. Zhong, K.Q. Sun, Y.C. Hong and B.Q. Xu, "Impacts of organic stabilizers on catalysis of Au nanoparticles from colloidal preparation," *Acs Catalysis*, vol. 4, no. 11, pp. 3982-3993, 2014.

[10] C. Prossl, M. Kubler, M.A. Nowroozi, S. Paul, O. Clemens and U. I. Kramm, "Investigation of the thermal removal steps of capping agents in the synthesis of bimetallic iridium-based catalysts for the ethanol oxidation reaction," *Phys Chem Chem Phys*, vol. 23, no. 1, pp. 563-573, Jan 6 2021, doi: 10.1039/d0cp04900j.

[11] D.M. Bezerra, I.W. Zapelini, K.N. Franke, M.E. Ribeiro and D. Cardoso, "Investigation of the structural order and stability of mesoporous silicas under a

humid atmosphere," *Materials Characterization*, vol. 154, pp. 103-115, 2019, doi: 10.1016/j.matchar.2019.05.032.

[12] L. López Pérez, E. R. H. van Eck and I. Melián-Cabrera, "On the hydrothermal stability of MCM-41. Evidence of capillary tension-induced effects," *Microporous and Mesoporous Materials*, vol. 220, pp. 88-98, 2016, doi: 10.1016/j.micromeso.2015.08.024.

[13] A. Ghasemi and H. Sanaeishoar, "An Efficient one-pot synthesis of 1H-Pyrazolo [1, 2-b] phthalazine-5, 10-dione derivatives using MCM-41," J*ournal of Chemical Reactivity and Synthesis*, vol. 9, no. 3, pp. 58-64, 2019.

[14] A. Ahmad, M. H. Razali, K. Kassim and K.A.M. Amin, "Synthesis of multiwalled carbon nanotubes supported on M/MCM-41 (M= Ni, Co and Fe) mesoporous catalyst by chemical vapour deposition method," *Journal of Porous Materials*, vol. 25, pp. 433-441, 2018.

[15] R. De Clercq , M. Dusselier, C. Poleunis, D.P. Debecker, L. Giebeler, S. Oswald, E. Makshina and B.F. Sels, "Titania-silica catalysts for lactide production from renewable alkyl lactates: structure–activity relations," *ACS Catalysis*, vol. 8, no. 9, pp. 8130-8139, 2018, doi: 10.1021/acscatal.8b02216.

[16] A. S. Al-Awadi, A.M. Toni, M. Alhoshan, A. Khan, J.P. Labis, A. Al-Fatesh, A. E. Abasaeed and S.M. Al-Zahrani, "Impact of precursor sequence of addition for one-pot synthesis of Cr-MCM-41 catalyst nanoparticles to enhance ethane oxidative dehydrogenation with carbon dioxide," (in English), *Ceramics International*, vol. 45, no. 1, pp. 1125-1134, Jan 2019, doi: 10.1016/j.ceramint.2018.10.002.

[17] Q. Sun, N. Wang and J. Yu, "Advances in catalytic applications of zeolite-supported metal catalysts," *Advanced Materials*, vol. 33, no. 51, p. e2104442, Dec 2021, doi: 10.1002/adma.202104442.

[18] A. Wróblewska, M. Kujbida, G. Lewandowski, A. Kamińska, Z. C. Koren and B. Michalkiewicz, "Epoxidation of 1, 5, 9-Cyclododecatriene with hydrogen peroxide over Ti-MCM-41 Catalyst," *Catalysts*, vol. 11, no. 11, p. 1402, 2021.

[19] H. Sekkiou, R. Hamacha, T. Ali-Dahmane, A. Morsli and A. Bengueddach, "The effect of the method of copper incorporation on the structure of Si-MCM-41 and Al-MCM-41," J*ournal de la Société Chimique de Tunisie*, vol. 15, pp. 93-99, 2013.

[20] P.H. Chao, W.C. C. Jean, H.-P. Lin and T.C. Tsai, "Intercalation of silanes by ion imprinting method for improving hydrothermal stability of mesoporous silica," *Catalysis Today*, vol. 212, pp. 175-179, 2013/09/01/ 2013, doi: 10.1016/j.cattod.2012.08.029.

[21] M. Song, C. Zou, G. Niu and D. Zhao, "Improving the hydrothermal stability of mesoporous silica SBA-15 by pre-treatment with $(NH_4)_2SiF_6$," *Chinese Journal of Catalysis*, vol. 33, no. 1, pp. 140-151, 2012/01/01/ 2012, doi: 10.1016/s1872-2067(10)60283-5.

[22] C. Jiang, A. Su, X. Li, T. Zhou and D. He, "Study on the hydrothermal stability of MCM-41 via secondary restructure," *Powder Technology*, vol. 221, pp. 371-374, 2012, doi: 10.1016/j.powtec.2012.01.028.

[23] Y. Luo, C. Miao, Y. Yue, W. Yang, W. Hua and Z. Gao, "Chromium oxide supported on silicalite-1 zeolite as a novel efficient catalyst for dehydrogenation of isobutane assisted by CO_2," *Catalysts*, vol. 9, no. 12, 2019, doi: 10.3390/catal9121040.

[24] Y. Luo, C. Wei, C. Miao, Y. Yue, W. Hua and Z. Gao, "Isobutane dehydrogenation assisted by CO_2 over silicalite-1-supported ZnO Catalysts: Influence of Support Crystallite Size," *Chinese Journal of Chemistry*, vol. 38, no. 7, pp. 703-708, 2020, doi: 10.1002/cjoc.202000042.

[25] A. S. Al-Awadi, A.M. El-Toni, S.M. Al-Zahrani, A.E. Abasaeed, M. Alhoshan, A. Khan, J.P. Labis and A. Al-Fatesh, "Role of TiO_2 nanoparticle modification of Cr/MCM41 catalyst to enhance Cr-support interaction for oxidative dehydrogenation of ethane with carbon dioxide," *Applied Catalysis A: General*, vol. 584, 2019, doi: 10.1016/j.apcata.2019.117114.

[26] T. Wan, F. Jin, X. Cheng, J. Gong, C. Wang, G. Wu and A. Liu, "Influence of hydrophilicity and titanium species on activity and stability of Cr/MWW zeolite catalysts for dehydrogenation of ethane with CO_2," *Applied Catalysis A: General*, vol. 637, 2022, doi: 10.1016/j.apcata.2022.118542.

[27] V. Elías, E. Sabre, K. Sapag, S. Casuscelli and G. Eimer, "Influence of the Cr loading in Cr/MCM-41 and TiO_2/Cr/MCM-41 molecular sieves for the photodegradation of Acid Orange 7," A*pplied Catalysis A: General*, vol. 413-414, pp. 280-291, 2012, doi: 10.1016/j.apcata.2011.11.019.

[28] S. Kilicarslan, M. Dogan and T. Dogu, "Cr incorporated MCM-41 type catalysts for isobutane dehydrogenation and deactivation mechanism," *Industrial & Engineering Chemistry Research*, vol. 52, no. 10, pp. 3674-3682, 2013, doi: 10.1021/ie302543c.

[29] R. S. Araújo, F. O. S. Costa, D. A. S. Maia, H. B. S. Ana and C. L. Cavalcante, "Synthesis and characterization of Al-and Ti-MCM-41 materials : Application To Oxidation Of Anthracene," 2007.

[30] A. Wróblewska, P. Miądlicki, J. Tołpa, J. Sreńscek-Nazzal, Z. C. Koren and B. Michalkiewicz, "Influence of the titanium content in the Ti-MCM-41 catalyst on the course of the α-pinene isomerization process," *Catalysts*, vol. 9, no. 5, p. 396, 2019.

[31] K. Sing, F. Schüth and T. Weitkamp, "Handbook of porous solids," Wiley, vol. 3, pp. 1543-1591, 2002.

[32] F.J. Sotomayor, K.A. Cychosz and M. Thommes, "Characterization of micro/mesoporous materials by physisorption: concepts and case studies," A*cc. Mater. Surf. Res*, vol. 3, no. 2, pp. 34-50, 2018.

[33] P. S. Niphadkar, S. K. Chitale, S. K. Sonar, S. S. Deshpande, P. N. Joshi and S. V. Awate, "Synthesis, characterization and photocatalytic behavior of TiO_2–SiO_2 mesoporous composites in hydrogen generation from water splitting," *Journal of Materials Science*, vol. 49, no. 18, pp. 6383-6391, 2014, doi: 10.1007/s10853-014-8365-2.

[34] S. K. Roy, D. Dutta and A. K. Talukdar, "Highly effective methylated Ti MCM-41 catalyst for cyclohexene oxidation," (in English), *Materials Research Bulletin*, vol. 103, pp. 38-46, Jul 2018, doi: 10.1016/j.materresbull.2018.03.017.

[35] A. Talati, M. Haghighi and F. Rahmani, "Impregnation vs. coprecipitation dispersion of Cr over TiO_2 and ZrO_2 used as active and stable nanocatalysts in oxidative dehydrogenation of ethane to ethylene by carbon dioxide," *RSC Advances*, vol. 6, no. 50, pp. 44195-44204, 2016, doi: 10.1039/c6ra05049b.

[36] Y. Liu, Y. Liu, A. Peyrav, Z. Hashisho, S. Zheng, Z. Sun, X. Chen, Y. Tong, Y. Hao and J. Wang, "Experimental and simulation investigation of water vapor adsorption on mesoporous MCM-41 derived from natural Opoka," (in English), *Separation and Purification Technology*, vol. 309, p. 123056, Mar 15 2023, doi: 10.1016/j.seppur.2022.123056.

[37] C. Gaidau, A. Petica, M. Ignat, L. M. Popescu, R.M. Piticescu, I.A. Tudor and R.R. Piticescu, "Preparation of silica doped titania nanoparticles with thermal stability and photocatalytic properties and their application for leather surface functionalization," (in English), *Arabian Journal of Chemistry*, vol. 10, no. 7, pp. 985-1000, Nov 2017, doi: 10.1016/j.arabjc.2016.09.002.

[38] K. Bourikas, C. Kordulis and A. Lycourghiotis, "Titanium dioxide (anatase and rutile): surface chemistry, liquid-solid interface chemistry, and scientific synthesis of supported catalysts," *Chem Rev*, vol. 114, no. 19, pp. 9754-823, Oct 8 2014, doi: 10.1021/cr300230q.

[39] A.D. Erdali, S. Cetinyokus and M. Dogan, "Investigation of isobutane dehydrogenation on $CrOx/Al_2O_3$ catalyst in a membrane reactor," *Chemical Engineering and Processing - Process Intensification*, vol. 175, p. 108904, May 1 2022, doi: 10.1016/j.cep.2022.108904.

[40] T. Ehiro, A. Itagaki, H. Misu, M. Kurashina, K. Nakagawa, M. Katoh, Y. Katou, W. Ninomiya and S. Sugiyamaet, "Oxidative dehydrogenation of isobutane to isobutene on metal-doped MCM-41 catalysts," J*ournal of Chemical Engineering of Japan*, vol. 49, no. 2, pp. 136-143, 2018.